CHAPTER 5

FABRICATION OF Mg/xMgO (x = 0, 5, 10, 15 %) COMPOSITES THROUGH A NOVEL SINTERING APPROACH

This chapter describes the fabrication of Mg/MgO composites through powder metallurgy employing a very cost effective sintering method. Pure Mg and Mg/MgO composites with varying weight fraction of 5, 10, and 15 % MgO reinforcement were fabricated by this process. The samples were characterised for density, porosity, hardness and compression tests. X - ray diffraction and microstructural characterisation were also done to study the phases and their distribution in the Mg matrix. Finally, the results are discussed on the effect of varying weight % of MgO reinforcements in pure Mg on different physical and mechanical properties.

5.1 Results

Magnesium based metal matrix composites have been synthesized over the years through many traditional routes namely casting, infiltration routes, powder metallurgy etc. Several new routes like Disintegrated Melt Deposition (DMD) technique, additive manufacturing, friction stir deposition etc. have also been successfully used for fabrication of Mg MMCs. In spite of many newly developed techniques, casting remains the most commonly employed process for Mg alloys and composites. Many newly developed techniques are being continuously improved and also new processes which are cost effective are still being searched especially for Mg MMCs.

In the present work, Mg composites were synthesized by powder metallurgy and different physical and mechanical properties were studied. Mg/MgO composites have been synthesized by both liquid state technique (casting, melt infiltration, in situ

techniques, etc.) and solid state techniques (Powder Metallurgy). Powder Metallurgy has been used by very few researchers for Mg/MgO composites. The details of entire processing method have been described in section 3.2.

5.2 Characterisation of Mg/xMgO (x = 0, 5, 10, 15 %) MMCs

5.2.1 Density and porosity of Mg/xMgO (x = 0, 5, 10, 15 %) MMCs

The density of the samples was measured by Archimedes principle as described in section 3.3.2. Table 5.1 shows the results of density and porosity of pure Mg and Mg/MgO composites. Figure 5.1 shows the variation of theoretical density, sintered density and porosity with respect to weight fraction of MgO in the composites.

Table 5.1 Results of density and porosity of pure Mg and Mg- MgO composites

Material	MgO (%)		Sintered Density (g/cm^3)	Theoretical Density (g/cm^3)	Relative Density (%)	Structural Porosity (%)
	(Wt.)	(Vol.)				
Mg/0MgO	0	0	1.69 ± 0.0004	1.738	97.04	2.95 ± 0.02
Mg/5MgO	5	2.49	1.73 ± 0.0004	1.783	97.23	2.76 ± 0.02
Mg/10MgO	10	5.11	1.80 ± 0.0004	1.832	98.16	1.84 ± 0.04
Mg/15MgO	15	7.89	1.81 ± 0.0004	1.883	96.19	3.81 ± 0.02

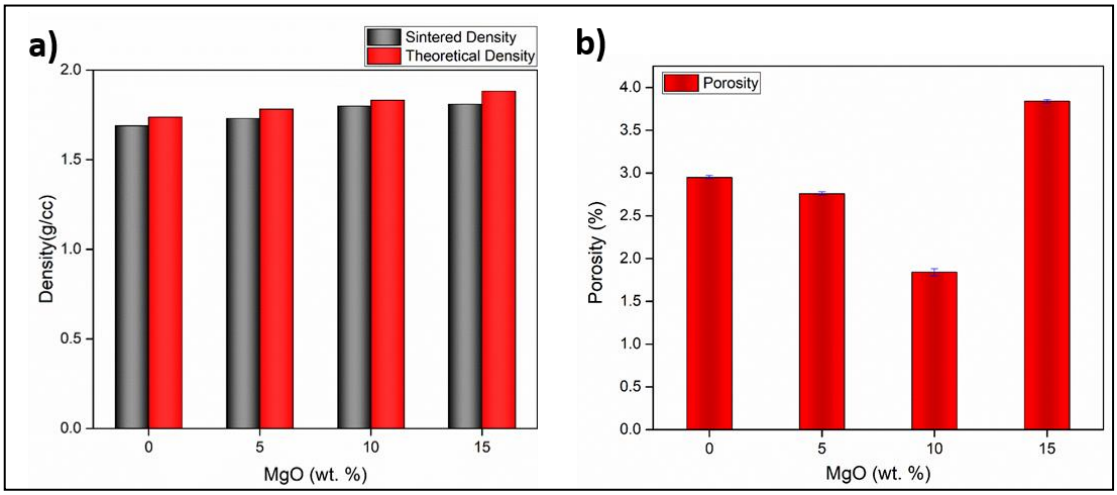

Figure 5.1 Effect of varying MgO content on a) sintered and theoretical density and b) porosity of Mg/MgO composites

The density of Mg and MgO particles is 1.738 g/cm^3 and 3.54 g/cm^3 respectively. It is observed from table 5.1 that when 5 wt. % MgO is added in pure Mg, the experimental density increases by 2.3% and when 10 wt. % MgO is added in pure Mg, the increases is 4.04% and only 0.5% increase in Mg/15MgO sample. The structural porosity of samples decreases by 6.4% with 5 wt. % MgO addition. It further decreases by 33.3 % in Mg/10MgO sample when compared to pure Mg and then sharply increases in 15 wt. % MgO sample as seen in the Figure 5.1(b). The maximum relative density of more than 98% was achieved for Mg/10MgO samples.

5.2.2 X – ray diffraction and microstructural characterisation of Mg/xMgO (x = 0, 5, 10, 15 %) MMCs

Phase identification and analysis of all the samples were done using X - ray diffraction technique using the high score plus software. Initially XRD of mixed powders as shown in Figure 5.2 were done to check the purity and compositional integrity of powders after mixing stage. It can be observed that Mg and MgO are the only phases present in XRD result and no other phases are formed during mixing. The figure also shows the absence of MgO peaks in pure Mg powder. However, as MgO is added in Mg/5MgO powder, a small peak appears in the pattern. As more MgO is added in Mg/10MgO and Mg/15MgO powders, the XRD pattern witnesses a corresponding increase in MgO peaks.

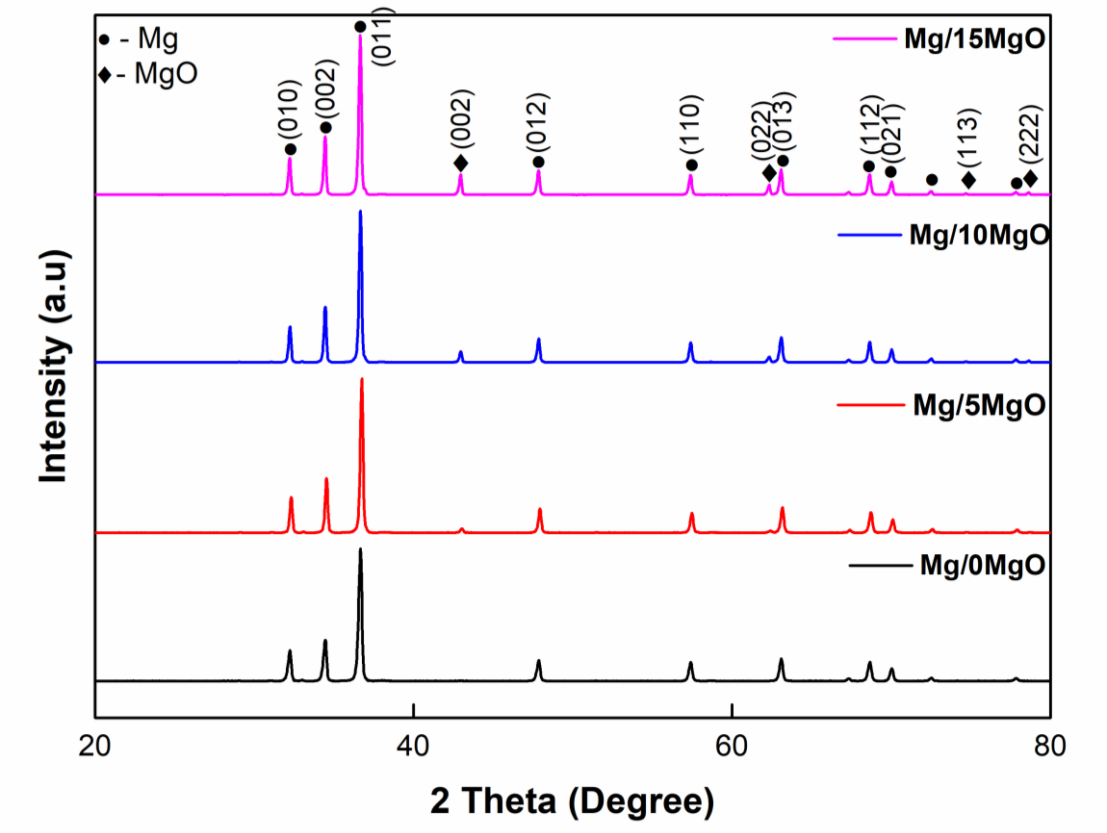

Figure 5.2 XRD pattern of Mg/0MgO, Mg/5MgO, Mg/10MgO and Mg/15MgO powders after mixing

Figure 5.3 shows the X - ray diffractograms of pure Mg and Mg/MgO composites after sintering is done. It can be observed that Mg and MgO are two phases present in composites. Phases other than these were not observed. Sharp peaks observed at 2θ angles 42.9°, 62.3°, 74.6° and 78.6° can be indexed to the cubic phase of MgO in all Mg/MgO composite samples. As the MgO weight fraction is increased in Mg/5MgO sample, the MgO peak appears in diffractograms. MgO peak intensity increases as further addition of MgO reinforcements is done in Mg/10MgO and Mg/15MgO samples. When we compare the XRD pattern of mixed powders with corresponding sintered sample, we observe that there in an increase in MgO intensity in sintered samples.

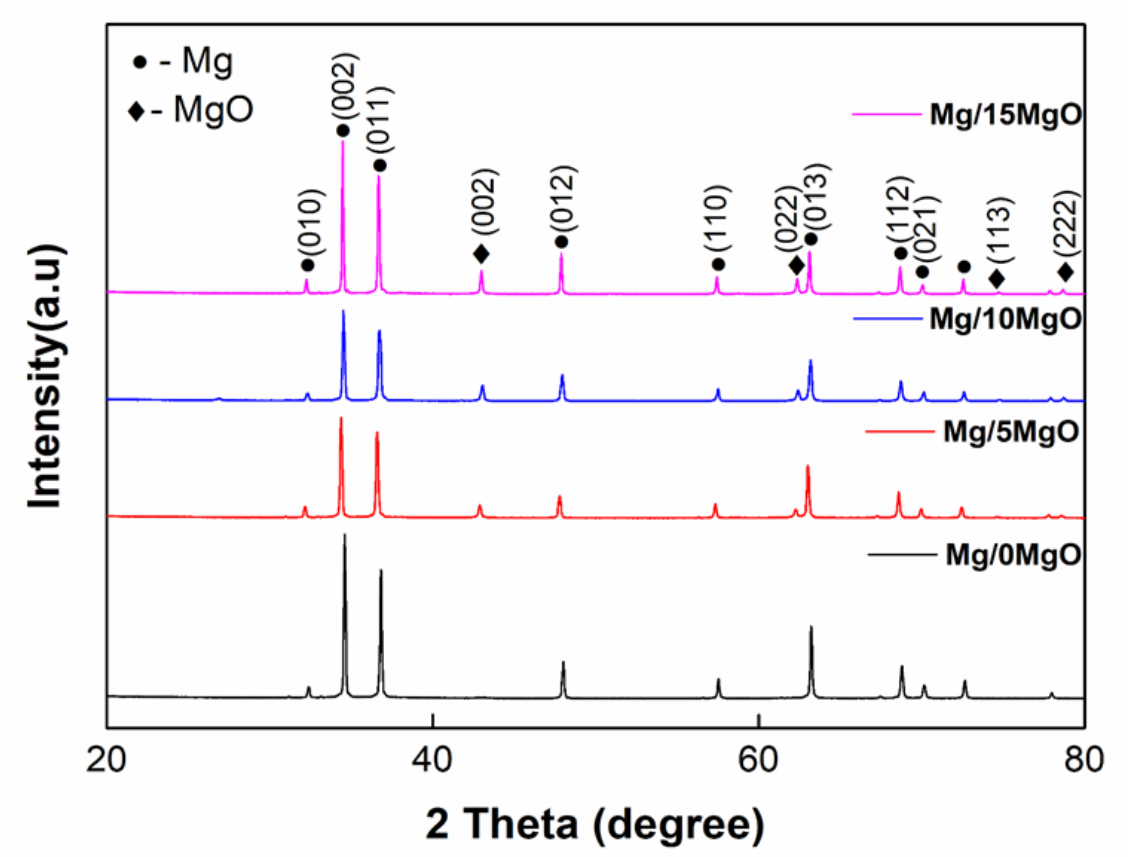

Figure 5.3 XRD patterns of Mg/0MgO, Mg/5MgO, Mg/10MgO and Mg/15MgO samples after sintering

The quantitative analysis of sintered samples were done using relative intensity method to calculate extra MgO phase formation during the sintering process and depicted in table 5.2. It is observed that Mg/0MgO has nearly 1.45 vol. %, Mg/5MgO has 2.81%, Mg/10MgO has 2.65 % and Mg/15MgO has 2.04 % increase in MgO formation.

Table 5.2. Comparison of vol. % of MgO formation before and after sintering

Material	MgO Vol (%) before sintering	MgO Vol (%) calculated in sintered samples	Increase in MgO vol. %
Mg/0MgO	0	1.45	1.45
Mg/5MgO	2.49	5.30	2.81
Mg/10MgO	5.11	7.76	2.65
Mg/15MgO	7.89	9.93	2.04

The results of average crystallite size and lattice strain calculated by Scherer's formula are listed in Table 5.3. The average crystallite size of Mg increases in Mg/5MgO when compared to Mg/0MgO. Then it decreases in Mg/10MgO and slightly increases in Mg/15MgO sample. The average lattice strain of Mg increases when 5 wt. % MgO is added to pure Mg. It again increases in Mg/10MgO and then slightly decreases in Mg/15MgO sample.

Table 5.3. Average Crystalline size and average lattice strain of all sintered composite

Material	Mg		MgO	
	Average Crystalline Size (nm)	**Average lattice strain (%)**	**Average Crystalline Size (nm)**	**Average lattice strain (%)**
Mg/0MgO	40.45 ± 09.67	0.05 ± 0.02	-	-
Mg/5MgO	54.44 ± 10.34	0.195 ± 0.17	47.12 ± 05.77	0.159 ± 0.05
Mg/10MgO	36.07 ± 04.86	0.217 ± 0.04	24.39 ± 04.59	0.225 ± 0.06
Mg/15MgO	38.64 ± 08.64	0.214 ± 0.01	32.38 ± 05.01	0.221 ± 0.03

The microstructural characterisation of pure Mg and Mg/MgO composites were done by SEM in both secondary electron (SE) mode and back scattered electron (BSE) mode. Figure 5.4 shows the microstructure of pure Mg and Mg/MgO composites in BSE mode at low magnification and Figure 5.5 shows the microstructure of specimens at high magnification. It can be inferred from the figures that micrographs of pure Mg and Mg/MgO composites shows predominantly two phases. The light phase is the Mg phase and dark grey phase is the MgO phase and black spots are pores. Fig 5.5 shows that the dark phases are mainly settled at grain boundary. Mg/15MgO micrograph in Figure 5.5 shows large agglomeration and clustering of MgO particles. Mg/15MgO micrograph also shows large number of pores than other samples. It is also observed that pore size increases in Mg/15MgO sample compared to other samples.

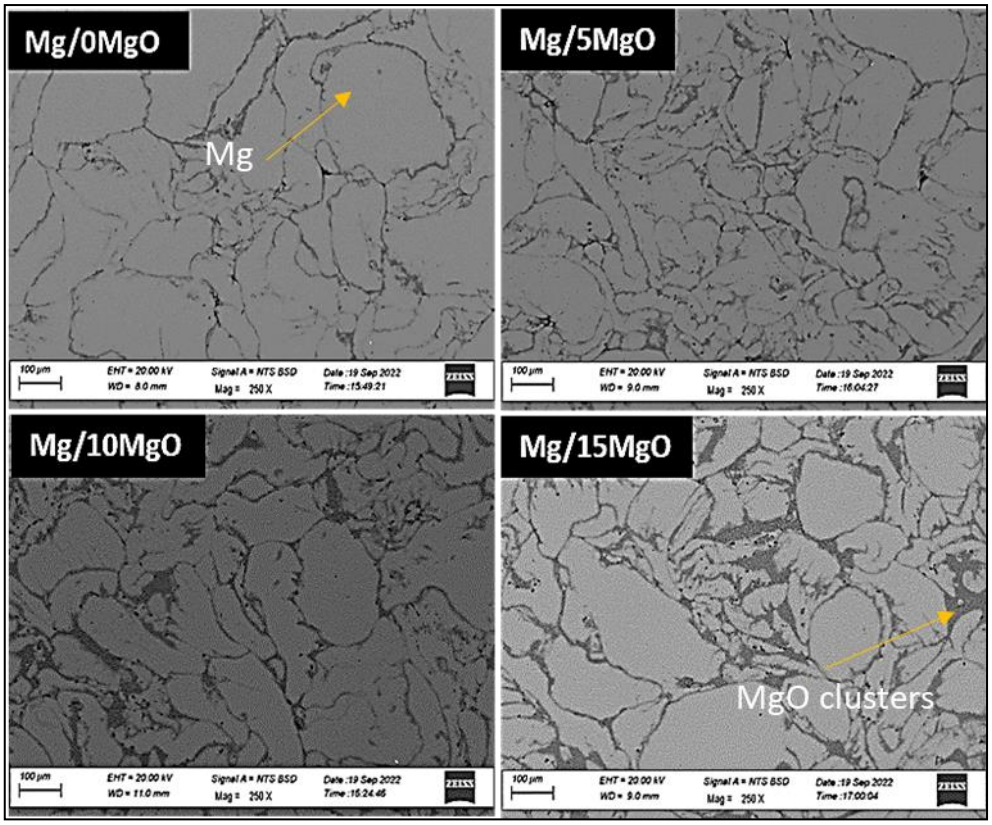

Fig 5.4 SEM micrographs of sintered composites at low magnification in BSE mode

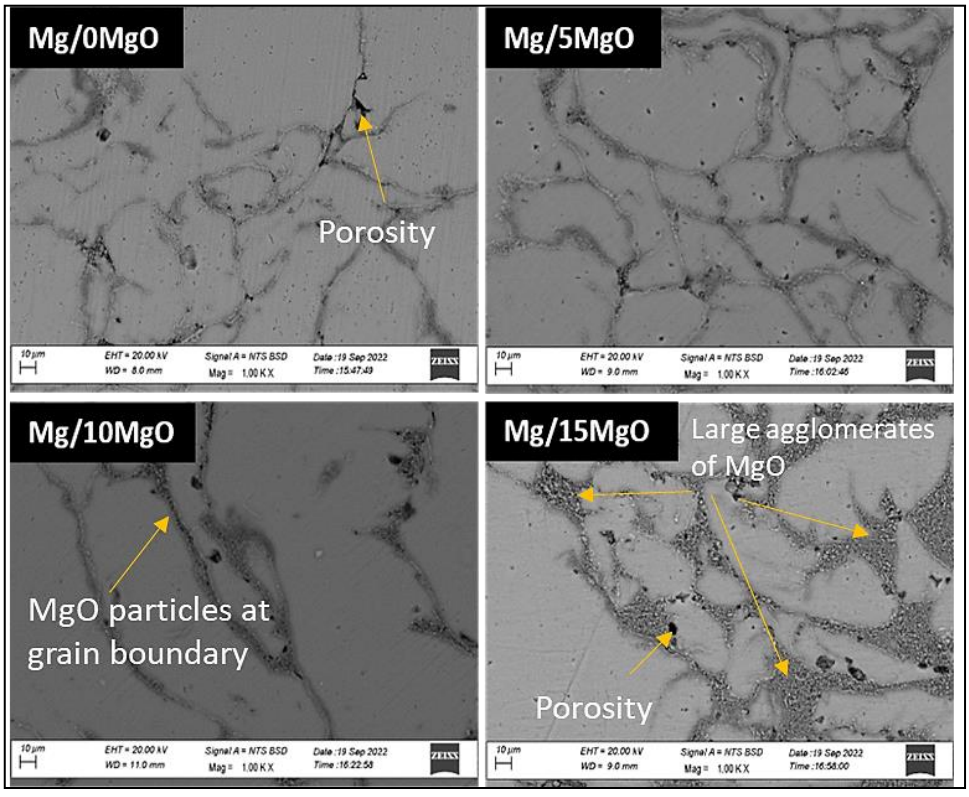

Fig 5.5 SEM micrographs of sintered composites at high magnification in BSE mode

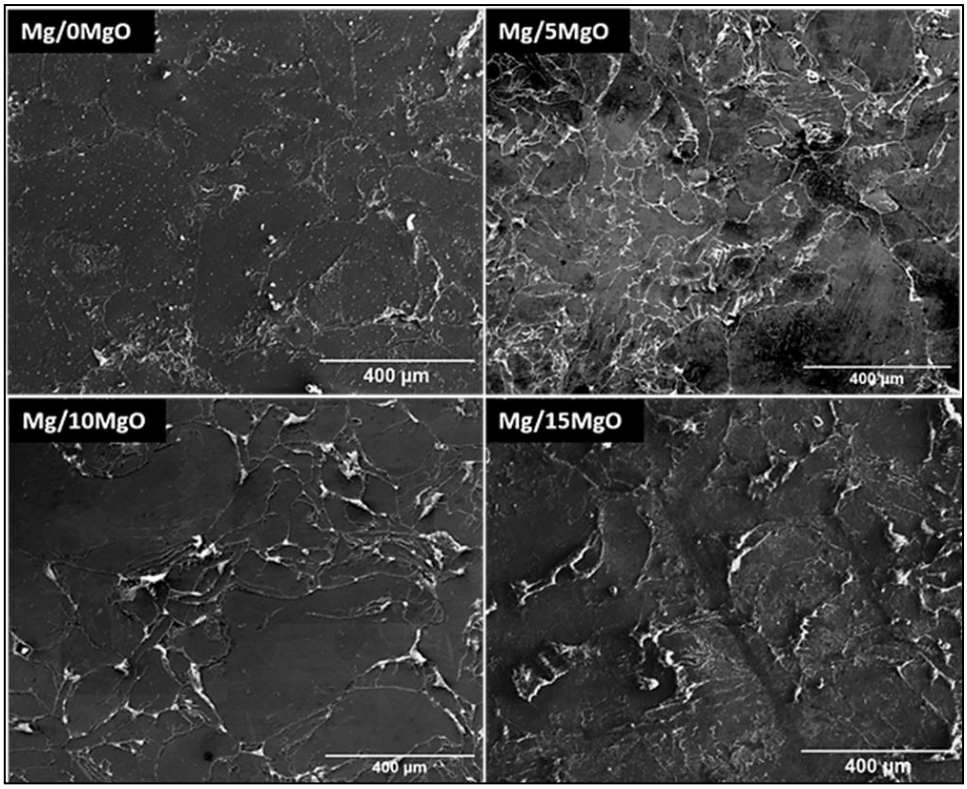

Fig 5.6 SEM micrographs of Mg/xMgO (x = 0, 5, 10, 15 %) MMCs at low magnification in SE mode

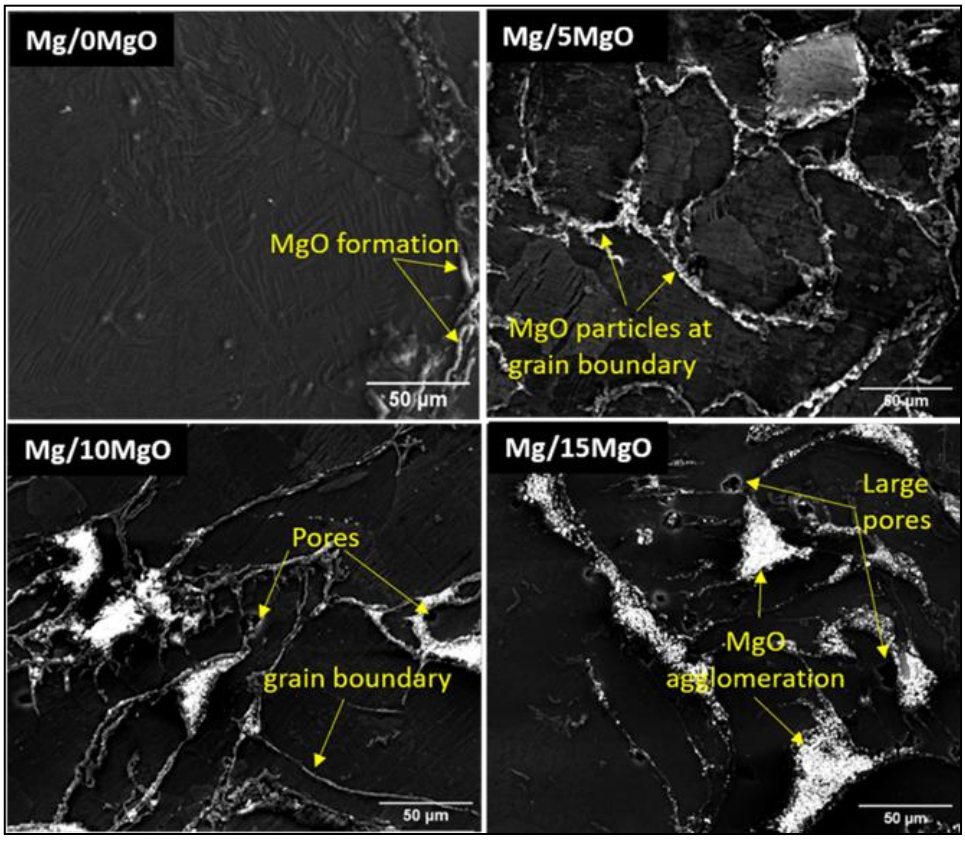

Fig 5.7 SEM micrographs of Mg/xMgO (x = 0, 5, 10, 15 %) MMCs at high magnification in SE mode

Figure 5.6 and 5.7 show the SEM micrographs of Mg/xMgO (x = 0, 5, 10, 15 %) MMCs at low and high magnification respectively. The dark phase represents the Mg phase and the white phase represents the MgO phase. The black spots are the pores. It is evident from the Figure 5.6 and 5.7 that MgO reinforcement are settled at the grain boundary in all the samples. The Mg/15MgO micrograph in Figure 5.7 has large agglomeration of MgO reinforcements. Therefore, both micrographs in SE and BSE mode helps us to confirm phase distribution.

The results of grain size measurement of Mg/xMgO (x = 0, 5, 10, 15 %) MMCs is shown in table 5.4 and its variation with respect to weight % of MgO in Mg matrix is shown in Figure 5.8. It is observed that the addition of MgO particles leads to refinement of grains in Mg/5MgO and Mg/10MgO samples. Further addition of MgO in Mg/15MgO caused coarsening of grains.

Table 5.4. Results of grain size of Mg/xMgO (x = 0, 5, 10, 15 %) MMCs

Material	Grain Size (µm)
Mg/0MgO	88 ± 2.1
Mg/5MgO	69 ± 1.4
Mg/10MgO	68 ± 1.2
Mg/15MgO	78 ± 1.8

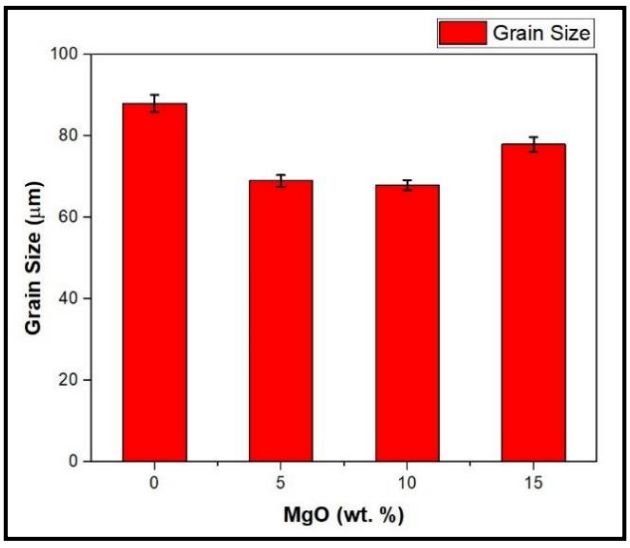

Figure 5.8 Grain size variation of Mg/xMgO (x = 0, 5, 10, 15 %) MMCs

Energy dispersive Spectroscopy (EDS) analysis was performed for composites. The elemental distribution (whole area scan and point scan of both phases) of Mg/5MgO and Mg/10MgO composites are shown in Figure 5.9 and Figure 5.10 respectively. The atomic and weight percentages are also shown in the same figures. Point scan of dark phase in both samples is Mg phase. The white phase in Figure 5.9 (c) and Figure5.10 (c) show both O and Mg element peaks which confirms it to be MgO phase.

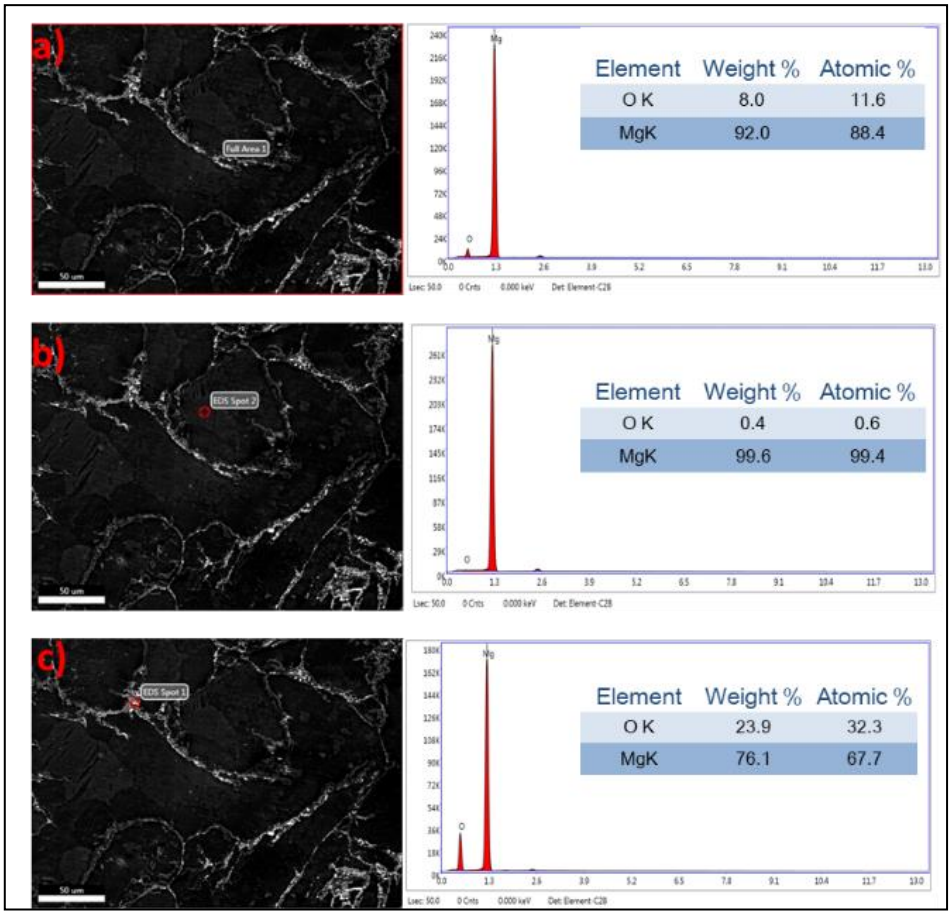

Figure 5.9 EDS elemental distribution of a) whole area scan, b) point scan at dark phase and c) point scan at light phase for Mg/5MgO composite

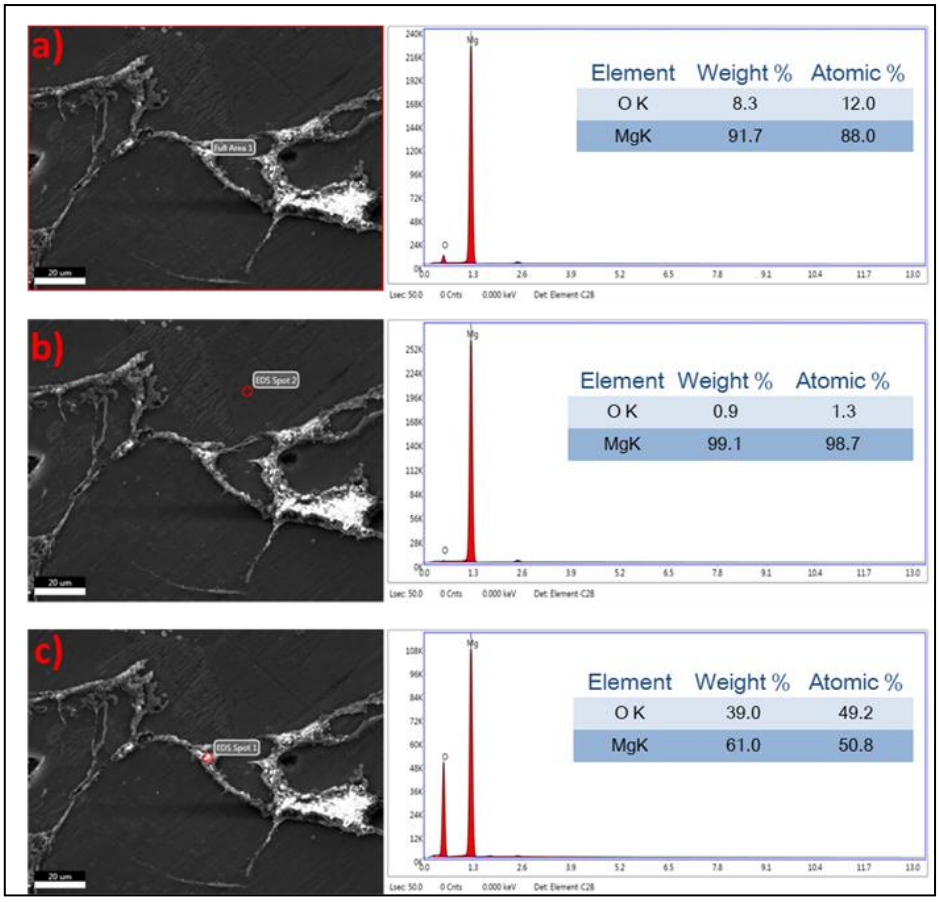

Figure 5.10 EDS elemental distribution of a) whole area scan, b) point scan at dark phase and c) point scan at light phase for Mg/10MgO composite

Figure 5.11, 5.12 and 5.13 shows the elemental mapping of selected area of Mg/5MgO, Mg/10MgO and Mg/15MgO composites. The elemental spectrum and weight % are also shown in the same figures. It is observed from the elemental maps that Mg and MgO phases are very distinctly separated. As the MgO content is increasing from 5 to 15 %, the weight % of O also increases simultaneously.

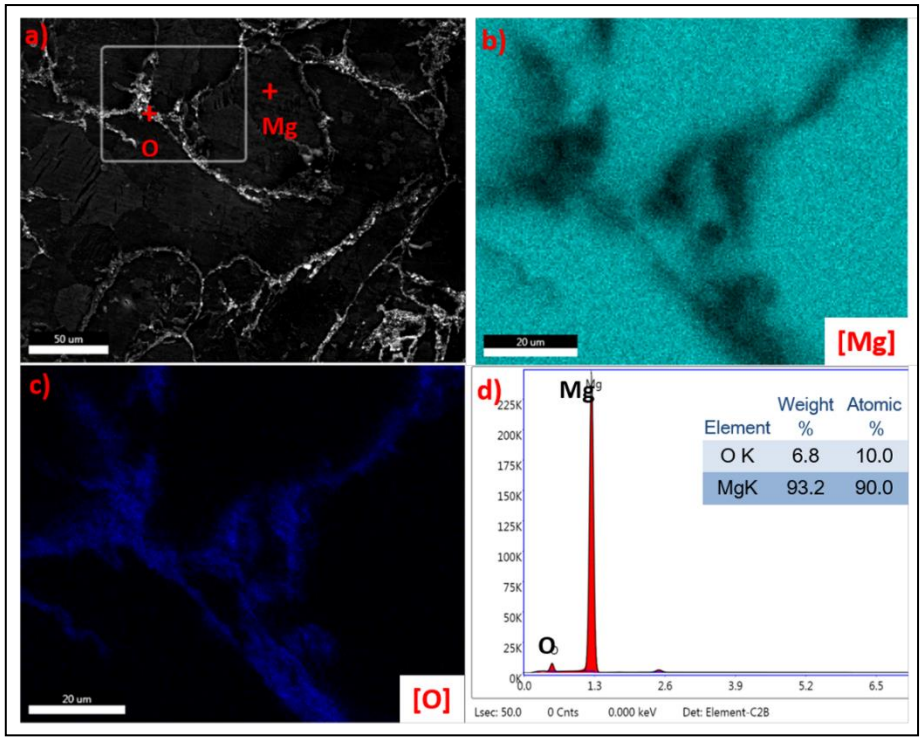

Figure 5.11 a) The SEM image of Mg/5MgO showing a) scanned area, EDS elemental map for b) Mg, (c) O, and (d) EDS spectrum along with elements percentage

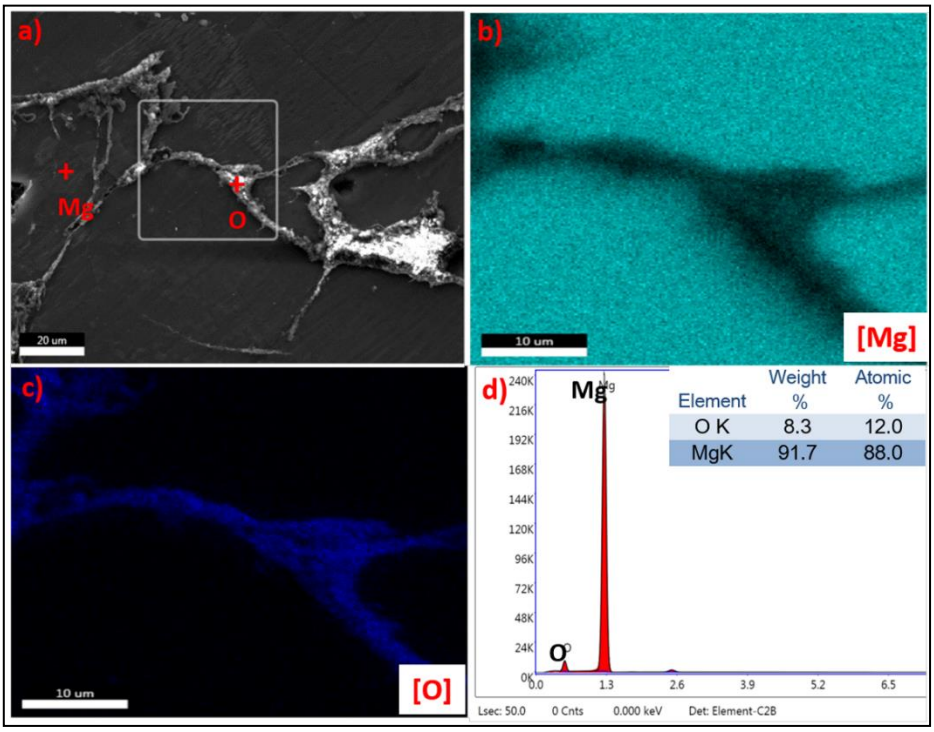

Figure 5.12 a) The SEM image of Mg/10MgO showing a) scanned area, EDS elemental map for b) Mg, (c) O, and (d) EDS spectrum along with elements percentage

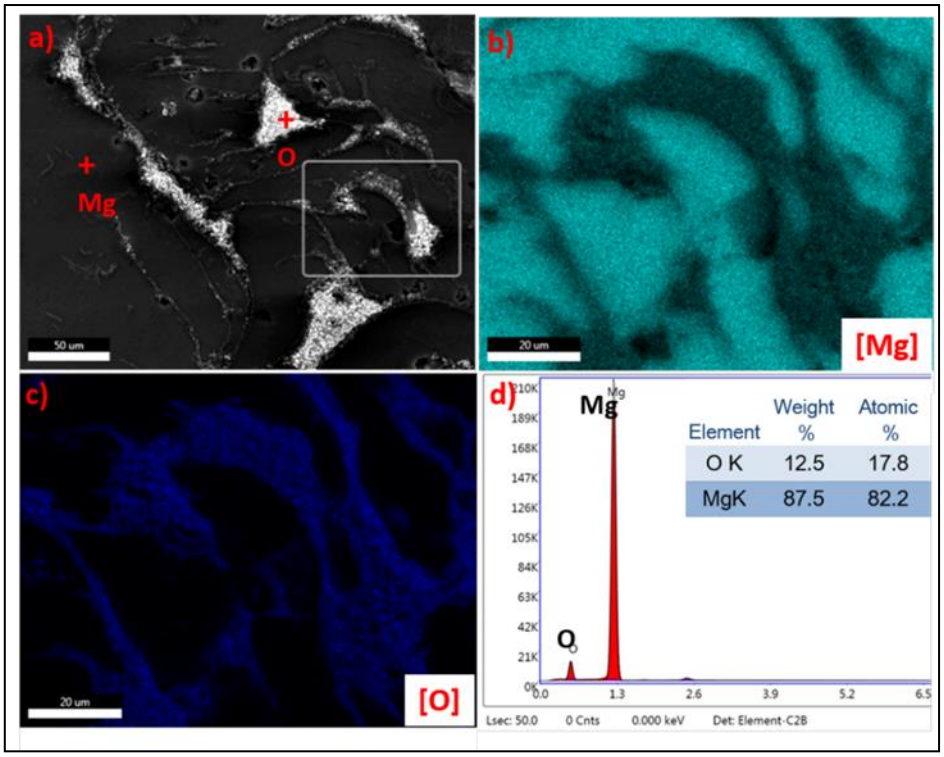

Figure 5.13 a) The SEM image of Mg/15MgO showing a) scanned area, EDS elemental map for b) Mg, (c) O, and (d) EDS spectrum along with elements percentage

Figure 5.14 shows the elemental line scanning done at an interface of Mg/10MgO composites which reveals elemental distribution at the interface. The elemental line scanning shows the depression in Mg profile and simultaneous rise in the O profile at the interface. The point where both Mg and O profile show sharp depression represents a pore at the interface.

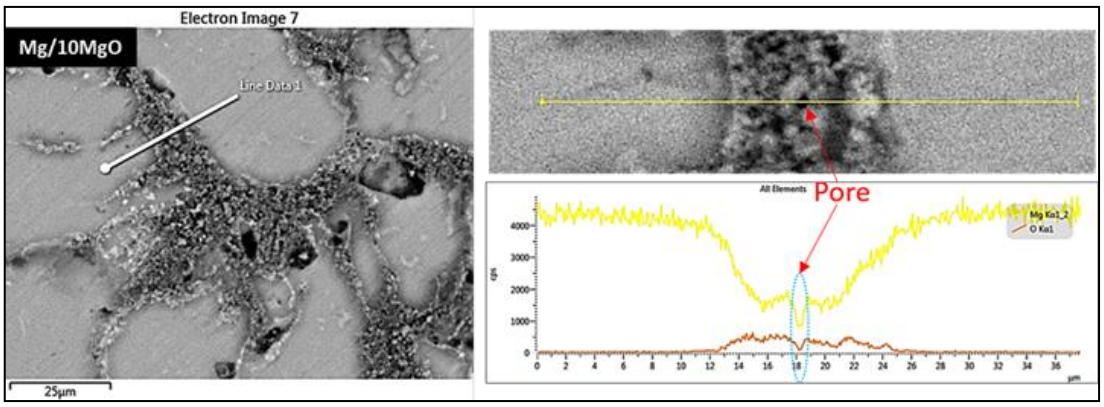

Figure 5.14 EDS line scanning done at the interface in Mg/10MgO sample

To ascertain the extent of oxidation of samples during sintering stage, an elemental line scanning was performed on the cross sectional area of all samples. The scanning was done over a distance of nearly 2000 μm from the periphery towards the core. The elemental line spectrum of all samples are shown in Figure 5.15.

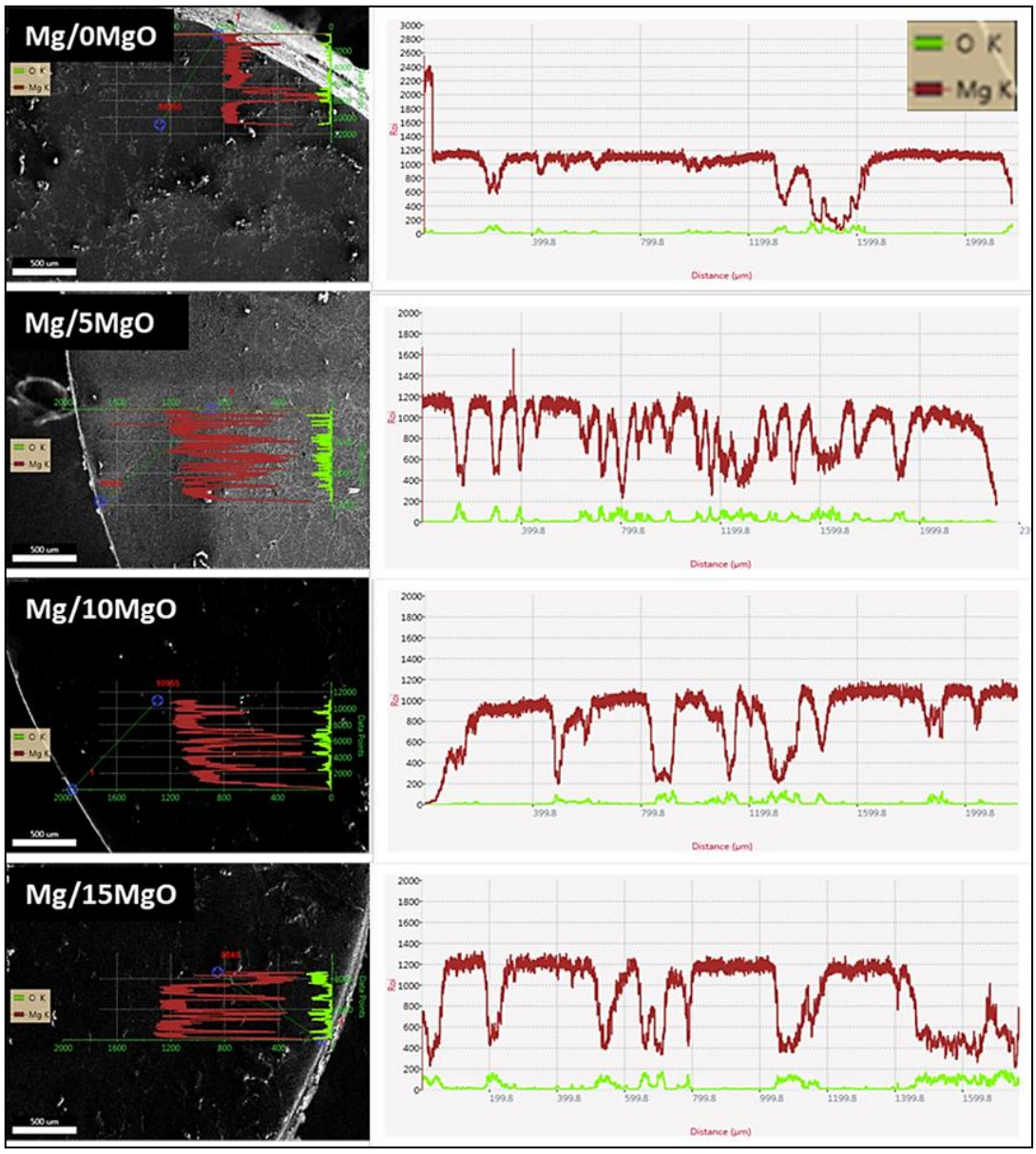

Figure 5.15 Line EDS scan of cross section from periphery towards core of each sample (Mg/0MgO, Mg/5MgO, Mg/10MgO and Mg/15MgO)

5.2.3 Hardness and compression test results of Mg/xMgO (x = 0, 5, 10, 15 %) MMCs

The results of the Vickers microhardness and room temperature compression test are listed in Table 5.5. The hardness variation with addition of different weight fractions of MgO is shown in Figure 5.16. The average hardness of composites increases gradually as the weight fraction of MgO increases. There is an increase of 9%, 13% and 29% hardness value with respect to pure Mg in Mg/5MgO, Mg/10MgO, and Mg/15MgO samples, respectively.

Table 5.5 Results of microhardness and room temperature compression testing

Material	0.2%CYS (MPa)	UCS (MPa)	Failure Strain (%)	Hardness ($HV_{0.05}$)
Mg/0MgO	65 ± 1.5	161 ± 1.9	18.0 ± 0.6	44 ± 4.9
Mg/5MgO	68 ± 1.7	172 ± 1.3	16.0 ± 0.4	48 ± 2.7
Mg/10MgO	80 ± 2.7	181 ± 2.1	13.5 ± 0.5	50 ± 5.3
Mg/15MgO	71 ± 2.1	144 ± 2.9	11.6 ± 0.5	57 ± 5.5

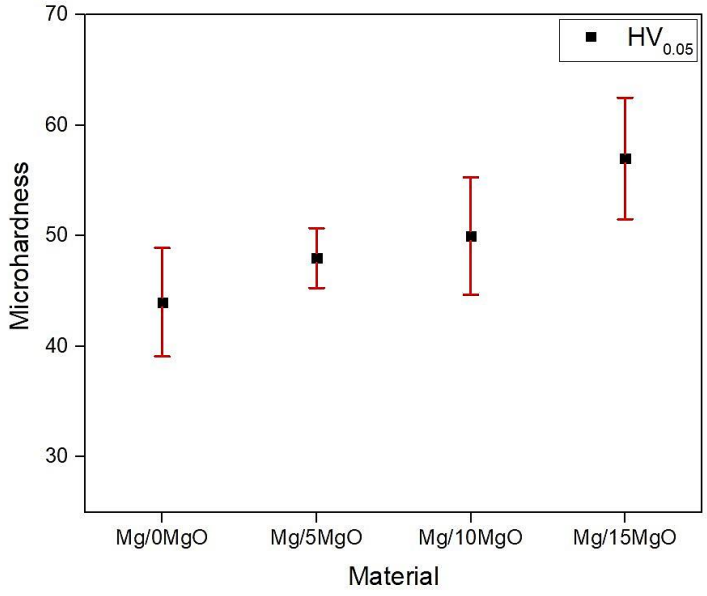

Fig 5.16 Microhardness of Mg/xMgO (x = 0, 5, 10, 15 wt. %) MMCs

The compressive stress-strain curve of Mg MMCs with change in wt. % of MgO reinforcement is shown in Figure 5.17. The variations of compressive yield stress (CYS), ultimate compressive strength (UCS) and failure strain with respect to weight fraction of MgO are shown in Fig 5.18. It illustrates that compressive yield strength increases with an increase in the weight fraction of MgO in Mg/5MgO and Mg/10MgO and then slightly decreases in Mg/15MgO. The increase in CYS is nearly 6% for Mg/5MgO and 23% for Mg/10MgO compared to pure magnesium. The UCS value improves in Mg/5MgO sample compared to pure Mg. Further improvement is observed in Mg/10MgO sample but in Mg/15MgO sample, UCS value drops sharply. The ductility of the sample decreases gradually as MgO content is increased in composites.

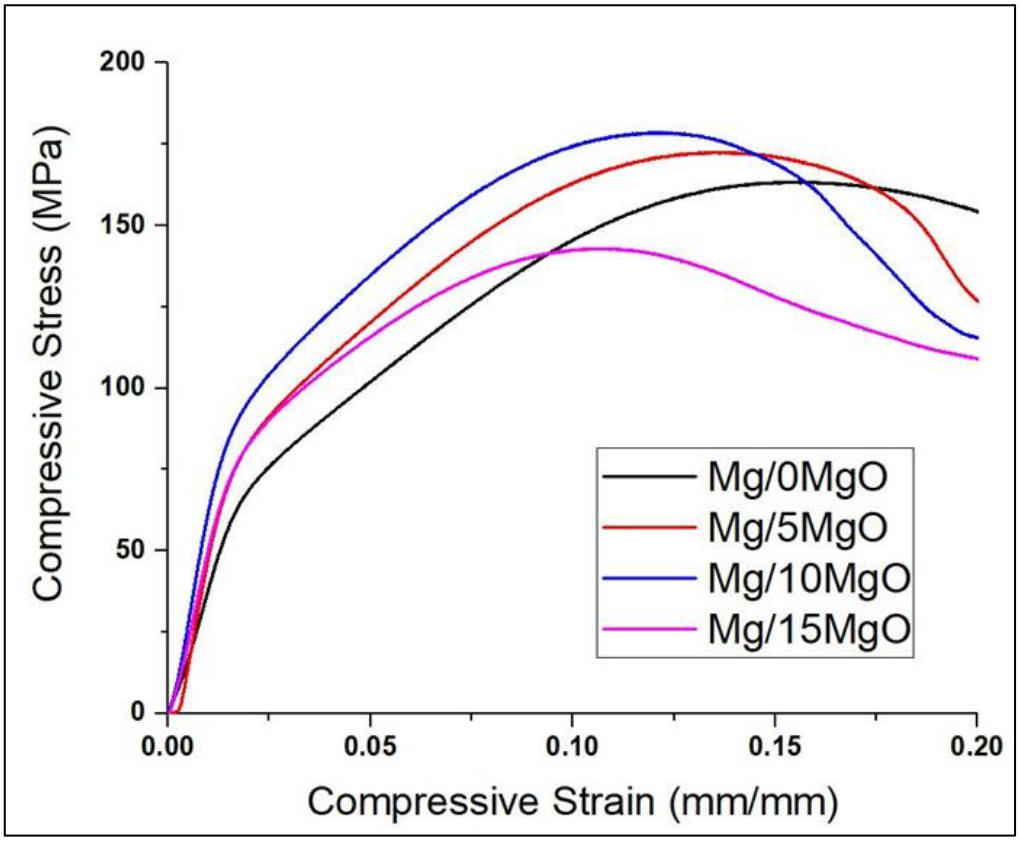

Figure 5.17 Compressive stress-strain curves of Mg/xMgO(x = 0, 5, 10, 15 wt %) composites

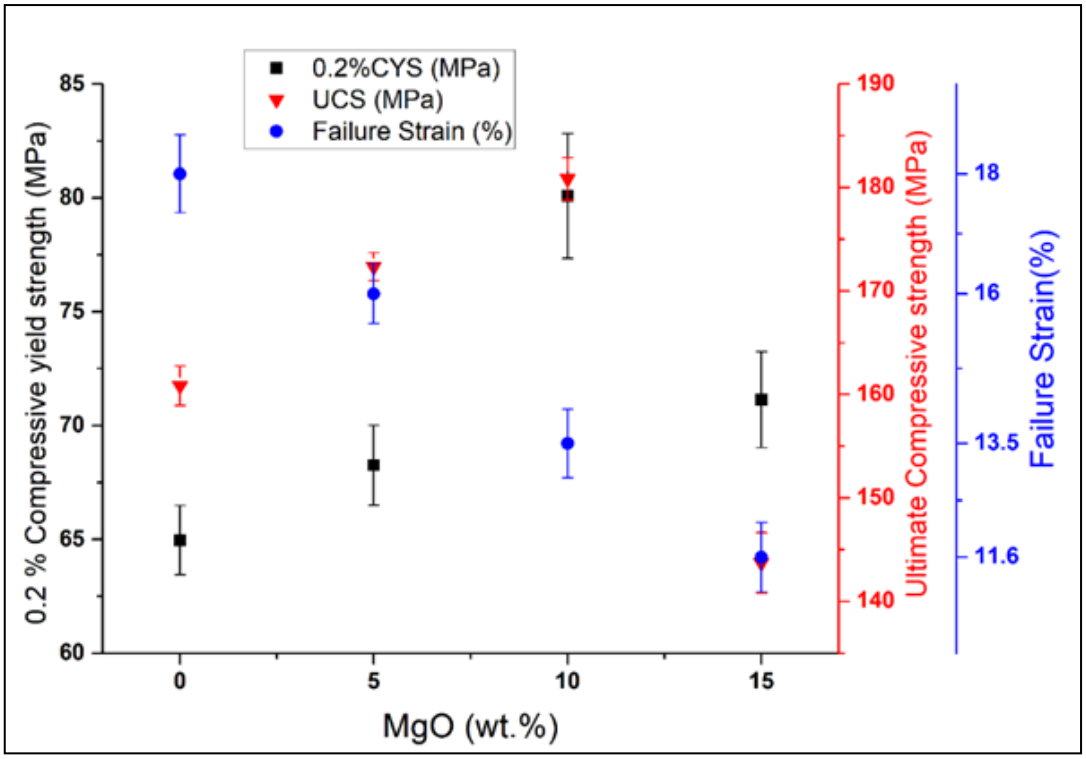

Figure 5.18 Variation of 0.2% CYS, UCS and failure strain with change in weight fraction of MgO in Mg/MgO MMCs

5.3 Discussion

In the first part of work pure Mg and Mg/MgO composites were fabricated by hybrid microwave sintering. The composite samples showed improvement in properties due to addition of MgO reinforcements. Mechanical properties were also improved. However, the porosity level were high in both pure Mg and Mg/MgO composites. This caused detrimental effect in the properties especially the degradation of mechanical properties. The main reasons were the quick heating rate of microwaves which induces high thermal stress at interface and the possibility of gas or vapour layer over powders which under high temperature tries to escape causing porosity.

The present fabrication method involves the sintering of composites in a muffle furnace with low heating rate of 5 °C/min. This reduces the thermal stresses at interfaces. In order to tackle the issue of gas or vapour layer over powders, initially MgO powders were preheated to 120°C for 2 hours in an oven before mixing with the Mg powders. The porosity level did not decrease. Fine cracks also appeared in the samples. The process was repeated several times still samples showed cracks. It was also observed that cracks mostly appeared in composites samples and not in pure Mg samples. One of the reason is that moisture still remains in the powder mixture which under high temperature comes out creating pores and cracks. To address the issue of moisture adsorption, thermo-gravimetric analysis (TGA) of mixed powder was done as mentioned in section 3.2.2.2. The TGA graph showing weight percentage change versus temperature for all samples is shown in Figure 5.19. The TGA of mixed powders were done from room temperature to 500 °C in order to observe any weight change in the range of sintering temperature.

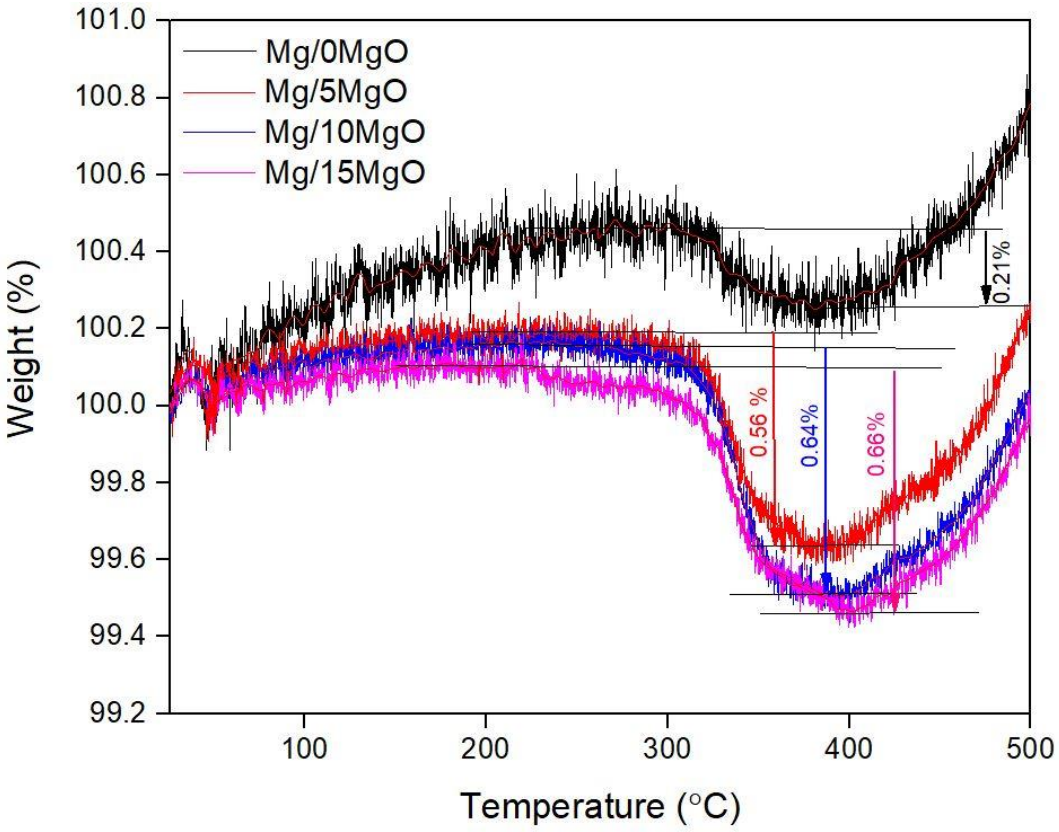

Figure 5.19 TGA graph showing weight percentage change vs temperature for Mg/0MgO, Mg/5MgO, Mg/10MgO and Mg/15MgO mixed powders.

It is observed from the Figure 5.19 that weight percentage change slightly increases in Mg/0MgO but remains nearly constant for composite powders up to temperature 300 °C. This is because the gas or vapour layer has high surface tension over the powder surface. As the temperature is further increased the weight of powders starts to decrease till temperature reaches slightly less than 400 °C. This weight reduction is nearly 0.21%, 0.56%, 0.64% and 0.66% for Mg/0MgO, Mg/5MgO, Mg/10MgO and Mg/15MgO, respectively. The weight reduction increases with increase in the MgO content in the composite. As the temperature is further increased and crosses 400 °C, weight gain starts to occur in all powders. This is because the Mg powders starts to oxidize above 400 °C.

Therefore, the preheating temperature of 120 °C which was earlier taken during trial experiments was not adequate. The preheating temperature was increased to 350 °C and the same process as described in section 3.2.2 was repeated. This change in preheating temperature was very crucial and resulted in sintered samples showing no sign of visible cracks and density of the samples also improved due to reduction in porosity.

The sintering of composites was done by covering the sample with an aluminium foil which acts as a protective cover and prevents oxidation. The melting point of aluminium is 660 °C and that of magnesium is 650 °C. The sintering of Mg or its alloys are usually done below 550 °C. Therefore, aluminium foil can protect the samples throughout sintering duration in this temperature range. The proper covering of Al foil on the samples is the key to achieve the best results. Many trial experiments were conducted on how to cover the aluminium foil over the sample so that oxidation doesn't takes place. It was concluded that 4 – 5 layer of wrapping is enough to cut off the sample from surrounding environment. The aluminium foil must be carefully wrapped so that it shouldn't get torn otherwise black protruding spot may appear as shown in fig 5.20(b). The sintering holding time was also varied to obtain the best holding time of 2 hours.

The sintered compacts after the removal of aluminium foil are shown in Figure 3.7 (a), and samples after coarse polishing are shown in Figure 3.7 (b). This method of sintering is mainly for small-size compacts as wrapping of large-size or complex shaped compacts in aluminium foil is not effective enough to separate the samples from the surrounding environment during sintering.

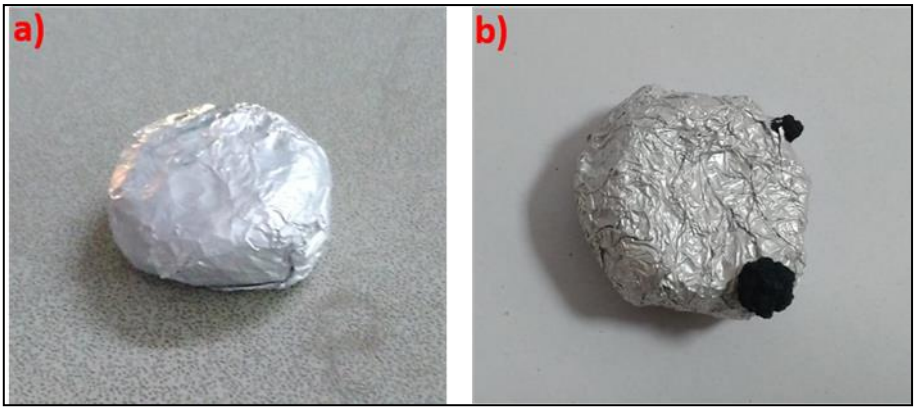

Figure 5.20 a) Sintered samples covered with Al foil taken out of furnace and b) sintered sample showing black protruding spots due to Al foil torn during wrapping

The sintered samples showed great improvement in density as shown in table 5.1. The density of Mg and MgO particles is 1.738 g/cm^3 and 3.54 g/cm^3 respectively. As MgO particles are mixed with Mg powders, density is definitely going to increase because the density of MgO is more than double the density of Mg. It can be seen in the Figure 5.7 that the high density MgO particle sits at the grain boundary of samples thereby reducing porosity which results in improvement in density. The rate of increase in density increases steadily up to 10 wt. % sample (Mg/10MgO) but when further MgO is added in Mg/15MgO sample, the increase in density rate drops sharply. This indicates the threshold limit of MgO addition in Mg matrix. The highest density was achieved for Mg/10MgO sample.

The structural porosity of samples decreases by 6.4% with 5 wt. % MgO addition. It further decreases by 33.3 % when 10 wt. % MgO is added and then sharply increases in 15 wt. % MgO sample. The reason for porosity in samples is firstly the inherent nature of powder metallurgy process wherein powders get welded together along with some gaps (pores) to get a denser product. Porosity is also due to adsorbed gas or moisture layer over powder surface but that had been tried to keep minimum. As MgO particles are added in pure Mg during compaction MgO particles sit between the gaps

of Mg particles thereby filling most of the voids in between and hence porosity reduces in Mg/5MgO sample. This can be seen in Figure 5.7, where white MgO particles sit at grain boundary and surround each Mg grains. As further 5 wt. % MgO is added in Mg/10MgO sample, more densification occurs and porosity again reduces. Further addition of MgO content sharply increases the porosity levels as shown in Figure 5.1(b). The sharp increase in the porosity in Mg/15MgO sample is mainly due to large agglomeration and clustering of MgO particles. It is also evident from microstructure of Mg/15MgO as shown in fig 5.7. Large pores are also visible which are mostly situated near the agglomeration areas in Mg/15MgO samples.

The X- ray diffractograms of mixed powders as shown in Figure 5.2 confirm that the purity and compositional integrity of powders are maintained after the mixing stage. The mixed powders do not show any peaks other than Mg and MgO which confirms that the powders are free from any impurities after the mixing stage and no additional compounds are formed. Mg/0MgO does not show any peak of MgO. As MgO content is increased in Mg/5MgO, Mg/10MgO, and Mg/15MgO powders, MgO peak also increases gradually. This confirms the gradual increase in MgO vol. fraction in the mixed powders. It also shows that powders have been mixed properly. The peak intensities of Mg and MgO at all diffraction planes did not change when compared to individual XRD patterns of Mg and MgO starting powders. This confirms the fact that mixing stage is free from any chemical interaction between the powders.

After the sintering is done, all samples show large changes in the diffraction peak intensity of Mg at all diffraction planes as seen in Figure 5.3. This is obvious as the recrystallization of grains occurs during sintering stage which changes the peak intensity of Mg at different planes. The XRD pattern of sintered samples also show only two phases. The major peaks are that of Mg and the minor peaks are of MgO.

Both the phases appear quite distinctly in the diffractograms and no other compounds were observed.

If we compare both the Figures 5.2 and 5.3 for each sample, we observe that MgO peaks at 42.9° and 62.3° 2θ angle increases in sintered samples than its corresponding powders. This means that vol. fraction of MgO slightly increases in sintered samples than the mixed powders for all compositions which indicated the possibility of oxidation of Mg into MgO. Upon doing the quantitative analysis of sintered samples for both phases, it was confirmed that some Mg particles oxidized to MgO during the sintering process. The results as listed in table 5.2 reveals that Mg/0MgO has nearly 1.45 vol. % increase in MgO formation. The increase in MgO vol. fraction in Mg/5MgO is nearly 2.81 %. Then there is decline in MgO formation in Mg/10MgO and Mg/15MgO samples. This phenomena of MgO formation during sintering of Mg based MMCs is common among researchers in spite of using best facilities. Many of them reported the same in their works [55, 87]. MgO formation has been reported even in Mg MMCs which do not contain MgO as reinforcement[49]. The formation of MgO during Mg fabrication is very difficult to avoid. This is because Mg is highly oxidative metal. Even in traces of oxygen, it will react to form MgO. The TGA results shown in Figure 5.19 also shows that above 400 °C only, weight increases due to oxidation of Mg into MgO. This tendency of MgO formation increases in powders metallurgy fabricated samples because Mg in powder form is more prone to oxidation.

The average crystallite size and average lattice strain have been shown in table 5.3. The results show that the average crystallite size increases with addition of 5 % MgO in pure MgO and decreases as more MgO is added in Mg/10MgO sample and remains nearly same for Mg/15MgO and lattice strain increases as the MgO content is increased. The decreasing crystallite size shows that adequate sintering occurred in the

samples. The lowest crystallite size is obtained for Mg/10MgO sample. The addition of hard MgO particulates settled at grain boundary increases the lattice strain in the composites.

The distribution of different phases can be easily observed in the scanning electron micrographs. MgO is difficult to focus in SEM, hence micrographs are taken in both BSE (Figure 5.4 and 5.5) and SE mode (Figure 5.6 and 5.7). The micrographs clearly show the distribution of only two phases. This supports the results of XRD phase analysis. XRD analysis showed only two (Mg and MgO) phases are present in sintered samples as discussed above. Upon elemental analysis as shown in Figure 5.9 and 5.10, it was confirmed that the light colour phase in BSE mode and dark colour phase in SE mode represents the Mg and dark colour phase in BSE mode and light colour phase in SE mode represents the MgO. Rahmani et al. also fabricated Mg/MgO composites by ECAP method and they also obtained similar microstructure [19]. The dark black spots in both BSE and SE mode represents pores. Pores are clearly visible in high magnification micrographs (Figure 5.5 and 5.7) in both BSE and SE mode. It is also seen from Figure 5.5 that pores are mostly situated at the interface of Mg grains. This is because bonding during sintering operations occurs due to necking between grains. At places where more grains meet, a void is formed creating a pore. This is an inherent nature of powder metallurgy products. Usually these pores are reduced by doing secondary processing like extrusion, rolling etc. The Mg/15MgO micrograph in Figure 5.5 and 5.7 show many large sized pores compared to other samples. It is also seen that all the pores lie at places where agglomeration of MgO particles has taken place. These pores degrade the strength of the Mg/15MgO composites.

The micrographs also give an idea about the distribution of MgO reinforcements in the Mg matrix. Figure 5.5 and 5.7 clearly show that the Mg/0MgO sample has almost

negligible MgO phase. Mg/5MgO and Mg/10MgO micrographs show evenly distributed MgO in the matrix. Mg/15MgO micrograph shows many clusters and agglomeration of MgO particulates. This indicates the threshold limit of MgO weight fraction in Mg matrix. The same micrographs also show that MgO particles are mainly situated at the grain boundaries of Mg matrix. MgO phase in not distributed in grains due to the negligible solid solubility of oxygen in the Mg matrix. Grain boundaries have high surface energy. Generally, grains grow to reduce this energy during the sintering process. But hard MgO particles present between the grains cause a strong pinning effect by resisting the movement of dislocations which eventually lead to the refinement of grains. This refinement of grain size increases the overall strength of composites. The grain size variation of each sample is shown in Figure 5.8. The addition of 5 wt. % MgO leads to considerable refinement in grains but when 10 wt. % MgO is added the decrease in grain size is very small. Addition of 15 wt. % MgO increases the grain size. This indicates that around 10 wt. % MgO is the threshold limit for the amount of MgO addition. In Mg/15MgO sample, agglomeration of MgO particles leads to uneven distribution of hard particles. Due to this, the pinning effect of hard particles weakens which leads to grain coarsening.

Energy Dispersive Spectroscopy (EDS) analysis was performed for composites. The elemental distribution (whole area scan and point scan of both phases) of Mg/5MgO and Mg/10MgO composites are shown in Figure 5.9 and Figure 5.10 respectively. The atomic and weight percentages of elements are also shown in the figures. Point scan in dark phase reveals only Mg peak in spectrum and point scan on light phase reveals both Mg and O peaks in the spectrum in both Mg/5MgO and Mg/10MgO samples. Therefore, the dark phase is Mg and the light phase is MgO. The elemental weight %

of Mg and O in both Mg/5MgO and Mg/10MgO samples are consistent with their respective compositional ratio.

The elemental map of Mg/5MgO, Mg/10MgO, and Mg/15MgO samples are shown in Figure 5.11, 5.12, and 5.13 respectively. These figures show the presence of only two elements Mg and O and no impurities were detected. It can be inferred that the MgO are predominantly distributed along the grain boundaries in Mg/5MgO and Mg/10MgO samples. Mg/15MgO sample shows many clusters of MgO particles. The elemental weight % of Mg and O in all the samples are nearly consistent with their respective compositional ratio.

The EDS elemental line scanning at the interface in Mg/10MgO as illustrated in Figure 5.14 reveals very clear demarcation of phase. The Mg spectrum is constant till the scanning is in Mg phase. As the line scanning enters the interface zone, the depression of Mg peak is observed with simultaneous increase in O peak. This indicates the presence of MgO in this zone. The point where both Mg and O spectrum drops represents a pore.

The EDS line scanning of elements were done for all the samples over a distance of nearly 2000 μm distance from outer surface towards core as illustrated in Figure 5.15. This was carried out in order check the extent of oxidation from outer surface towards the centre of sample. The figure shows that Mg spectrum has a constant peak intensity throughout the scanning distance. The profile do not show any continuous rising or falling trend. The peak intensity of O elemental in the spectrum is negligible for most of scanning distance in all the samples. The O line intensity do not show any rising trend over the distance. Only at places where line scan crosses the grain boundary or MgO particle there is decrease in Mg profile with simultaneous appearance of O peak.

In Mg/0MgO sample, the depression in Mg profile is observed at very few place due to very low content of MgO phase. The distance between O peaks is large. The Mg/5MgO sample shows depression in Mg profile in several numbers at short distances. It is also observed that at every depression of Mg profile there is appearance of O peak indicating it to be the MgO phase. This means that MgO phase which is settled at grain boundary as confirmed by microstructure in Figure 5.7 (Mg/5MgO) occurs at interval of short distances during elemental line scanning. This shows that the area where line scanning is performed contains many small sized grains in Mg/5MgO sample. In Mg/10MgO sample, the line spectrum shows Mg depression at larger distance with O peak at each depression and nearly same is observed in Mg/15MgO sample. The major difference between Mg/10MgO and Mg/15MgO EDS results is that the O peaks in Mg/10MgO sample occurs for very short distance than Mg/15MgO sample. This is because the Mg/15MgO contains many agglomerations of MgO reinforcements as seen in Figure 5.7. As line scanning passes over these pockets of agglomerates, O peaks continuously appears for larger distance. The results showed that oxidation did not occur at the outer surface of the samples. Hence, the chances of oxidation using the present method of sintering is minimal.

MgO is a hard ceramic having high compressive strength. When the fine particles of MgO are mixed with Mg, it surely improves the mechanical property of the fabricated MMC. This is evident from the table 5.5 which shows the results of hardness and compressive tests. The hardness value of composites increases as the MgO content increases in the Mg matrix as illustrated in Figure 5.16. The reason for significant improvement is firstly due to high hardness of MgO particles which are settled at grain boundaries. These hard MgO reinforcements resist the localised deformation of material during indentation. Secondly, the smaller grains due to grain refinement effect

also acts as constraint to localised surface deformation and hence improves the hardness value. The results are consistent with the findings of previous works on similar materials[19].

The compressive strength also increases due to addition of MgO reinforcements in the Mg matrix. It is seen from Figure 5.18 that the average compressive yield strength value marginally increases in Mg/5MgO with respect to pure Mg. Further improvement occurs in Mg/10MgO sample but the CYS value declines in Mg/15MgO. There are several reasons for the same. The elastic modulus of Mg is lower than that of MgO. So, when a composite is under loading condition, the Mg matrix enters the plastic zone at a certain threshold load. However, MgO particles are still in the elastic zone. So, if interfaces are assumed to be strong, MgO particle resists the plastic deformation of Mg and dislocation density increases around MgO particles. The large mismatch of coefficient of thermal expansion between Mg and MgO also generates large number of dislocations near the interface. This results in high dislocation density around MgO particles which in turn increases the strength of composite.

As the reinforcement weight fraction increases and distribution of reinforcement is homogeneous, the separation between MgO particles decreases which further enhances the dislocation density near MgO particles. So, movement of dislocations requires more stress and hence strength increases. Another factor for improvement of CYS is the load bearing capacity of reinforcement in Mg matrix. MgO is a hard ceramic having high compressive strength of 1.44 GPa [88]. The homogenous distribution of MgO particles in the Mg matrix increases the load-bearing effect of the matrix. The absence of cracks near the Mg-MgO interface increases the interfacial strength which further facilitates the load-bearing effect thereby increasing CYS. Orowan strengthening also improves the CYS of MMCs but its effect is more

dominant in nano sized reinforcing particles. The grain refinement due to MgO particles increases the grain boundaries in the material. This increases the overall strength of composites as grain boundaries resist the dislocation propagation. The detrimental factors for CYS are the porosities at interfaces which create discontinuity and weak interfacial bonding. Due to this, dislocation annihilation may take place sometimes due to absorption of dislocation if interfaces are weak.

In the present study, the increase in CYS value is nearly 6% for Mg/5MgO and 23% for Mg/10MgO compared to pure magnesium. This increase in CYS value is less in Mg/5MgO composite because there is small reduction in porosity value compared to pure Mg. Grain refinement effect does not influences much as its values are very close for Mg/5MgO and Mg/10MgO sample. In Mg/10MgO sample, porosity decreases sharply than Mg/5MgO. In addition, maximum MgO content accommodation takes place without clustering in Mg/10MgO. Hence, CYS improvement due to dislocation pile up and load bearing effect is maximum in Mg/10MgO sample. Further MgO addition in Mg/15MgO sample crosses the threshold limit for homogeneity and agglomeration and clustering is seen in microstructure (Figure 5.8). This results in sharp increase in porosity as is observed in Figure 5.1 (b). MgO particles come in direct contact with each other and weak bonding between MgO particles decreases the CYS value.

The UCS value increases steadily as the MgO weight fraction is increased in Mg/5MgO and Mg/10MgO samples. Further, MgO addition in Mg/15MgO sample results in low UCS value. This drop in UCS value is due to presence of large size pores mainly at the interfaces which under high load becomes vulnerable to crack initiation.

Ductility of samples decreases gradually as the MgO weight fraction is increased as depicted in Figure 5.18. Ductility in MMCs decreases mainly because of weak interfacial strength, presence of discontinuity like pores or voids etc. Mg/0MgO sample has highest ductility because it does not contain MgO particles. The micro plasticity must have in the metal matrix composites due to the stress concentration of the matrix at the pores of the reinforcement and or sharp corners of the reinforcing particle.

Therefore, Mg/MgO MMCs were successfully fabricated by the powder metallurgy using cost effective sintering technique. The increase in preheating temperature of MgO particles surely improved the density of composites which improved the overall strength and ductility of composites.

5.4 Conclusions

Based on the above results and discussion, following conclusions may be drawn:

- The Mg/MgO composites with varying weight fraction of 0, 5, 10, and 15 % of MgO were successfully fabricated using a novel sintering approach. The attempt to employ carefully wrapped aluminium foil on samples to effectively prevent oxidation from the surrounding environment was successful during the entire sintering duration.
- The density increases with increase in MgO content. Composites samples were nearly 97% and 98% dense for 5 and 10 wt. % MgO, respectively. The highest density was achieved for Mg/10MgO sample. The structural porosity of samples decreases by 6.4% with 5 wt. % MgO addition. It further decreases by 33.3 % when 10 wt. % MgO is added and then sharply increases in 15 wt. % MgO sample.

- XRD results reveals the presence of only Mg and MgO phase in composites. The quantitative analysis of phases showed extra MgO formation in all the samples during sintering because Mg is highly oxidative metal.
- MgO particles are mostly settled at grain boundaries and are uniformly dispersed in the Mg matrix. Clustering at few places was observed in Mg/15MgO sample. Grain size measurement showed decrease in size of grains as MgO content is increased up to Mg/10MgO thereafter it increases in Mg/15MgO.
- The composites showed an increasing trend in hardness value with an increase in MgO volume fraction. There is an increase of 9 %, 13 % and 29 % hardness value with respect to pure Mg in Mg/5MgO, Mg/10MgO, and Mg/15MgO samples, respectively.
- The CYS improves nearly 6 % for Mg/5MgO and 23 % for Mg/10MgO compared to pure magnesium. Further MgO incorporation in Mg/15MgO sample resulted in decrease in CYS value. The UCS value improves in Mg/5MgO sample compared to pure Mg. Further improvement is observed in Mg/10MgO sample but in Mg/15MgO sample, UCS value drops sharply. The ductility of the sample decreases gradually as MgO content is increased in composites.